

RESEARCH OUTPUTS / RÉSULTATS DE RECHERCHE

The role of geometry in nanoscale rectennas for rectification and energy conversion

Miskovsky, N. M.; Cutler, P. H.; Mayer, A.; Willis, B. G.; Zimmerman, D. T.; Weisel, G. J.; Chen, James M.; Sullivan, T. E.; Lerner, P. B.

Published in:

Proceedings of SPIE - The International Society for Optical Engineering

DOI:

[10.1117/12.2024187](https://doi.org/10.1117/12.2024187)

Publication date:

2013

Document Version

Publisher's PDF, also known as Version of record

[Link to publication](#)

Citation for pulished version (HARVARD):

Miskovsky, NM, Cutler, PH, Mayer, A, Willis, BG, Zimmerman, DT, Weisel, GJ, Chen, JM, Sullivan, TE & Lerner, PB 2013, The role of geometry in nanoscale rectennas for rectification and energy conversion. in *Proceedings of SPIE - The International Society for Optical Engineering*. vol. 8824, 88240P, Next Generation (Nano) Photonic and Cell Technologies for Solar Energy Conversion IV, San Diego, California, United States, 25/08/13.
<https://doi.org/10.1117/12.2024187>

General rights

Copyright and moral rights for the publications made accessible in the public portal are retained by the authors and/or other copyright owners and it is a condition of accessing publications that users recognise and abide by the legal requirements associated with these rights.

- Users may download and print one copy of any publication from the public portal for the purpose of private study or research.
- You may not further distribute the material or use it for any profit-making activity or commercial gain
- You may freely distribute the URL identifying the publication in the public portal ?

Take down policy

If you believe that this document breaches copyright please contact us providing details, and we will remove access to the work immediately and investigate your claim.

The Role of Geometry in Nanoscale Rectennas for Rectification and Energy Conversion

N. M. Miskovsky^{a,b}, P. H. Cutler^{a,b}, A. Mayer^c, B. G. Willis^e, D. T. Zimmerman^e, G. J. Weisel^e, James M. Chen^f, T. E. Sullivan^g, and P. B. Lerner^b

^a*Department of Physics, 104 Davey Laboratory, The Pennsylvania State University, University Park, Pennsylvania 16802, USA*

^b*Scitech Associates, LLC, 232 Woodland Drive, State College, Pennsylvania 16803, USA*

^c*Facultés Universitaires Notre-Dame de la Paix, Rue de Bruxelles 61, 5000 Namur, Belgium*

^e*Chemical, Materials & Biomolecular Engineering Department, University of Connecticut, Storrs, Connecticut 06269, USA*

^f*Division of Mathematics and Natural Sciences, 101 Elm Bldg., Pennsylvania State University, Altoona College, Pennsylvania 16601, USA*

^j*Division of Business and Engineering, Pennsylvania State University, Altoona college, PA*

^g*Department of Electrical & Computer Engineering, Temple University, Philadelphia, Pennsylvania 19122, USA*

1. INTRODUCTION

We have previously presented a method for optical rectification that has been demonstrated both theoretically and experimentally and can be used for the development of a practical rectification and energy conversion device for the electromagnetic spectrum including the visible portion. This technique for optical frequency rectification is based, not on conventional material or temperature asymmetry as used in MIM or Schottky diodes, but on a purely geometric property of the antenna tip or other sharp edges that may be incorporated on patch antennas. This “tip” or edge in conjunction with a collector anode providing connection to the external circuit constitutes a tunnel junction. Because such devices act as both the absorber of the incident radiation and the rectifier, they are referred to as “rectennas.” Using current nanofabrication techniques and the selective Atomic Layer Deposition (ALD) process, junctions of 1 nm can be fabricated, which allow for rectification of frequencies up to the blue portion of the spectrum (see Section 2).

In this paper we treat in detail the role of geometry in nanoscale rectennas for rectification and energy conversion. We also discuss different model analyses and mathematical treatments for electron emission from a sharp tip, which all exhibit the same focusing and tunneling features due to asymmetrical geometry.

Due to the incident radiation AC currents are induced along the length of the antenna, which produce oscillating charges at the top or edge of the geometrically asymmetric tunneling junction and corresponding image currents in the anode. The presence of the constricted geometry of the tip or edge gives rise to an enhanced field at the tip. The oscillating charges in the tunnel junction induce an AC voltage across the gap. If the induced field is sufficient for field emission, a tunneling current is produced. Due to geometric asymmetry (and possible material asymmetry or plasmonic coatings), there is a difference between the potential barriers for forward and reverse bias, which results in a rectified DC current (see section 3).

An SEM image of our fabricated geometrically-asymmetric device that we use in our own research is shown in Fig. 1. Note that we have chosen a device structure that has been fabricated on a large scale using standard nanofabrication techniques.

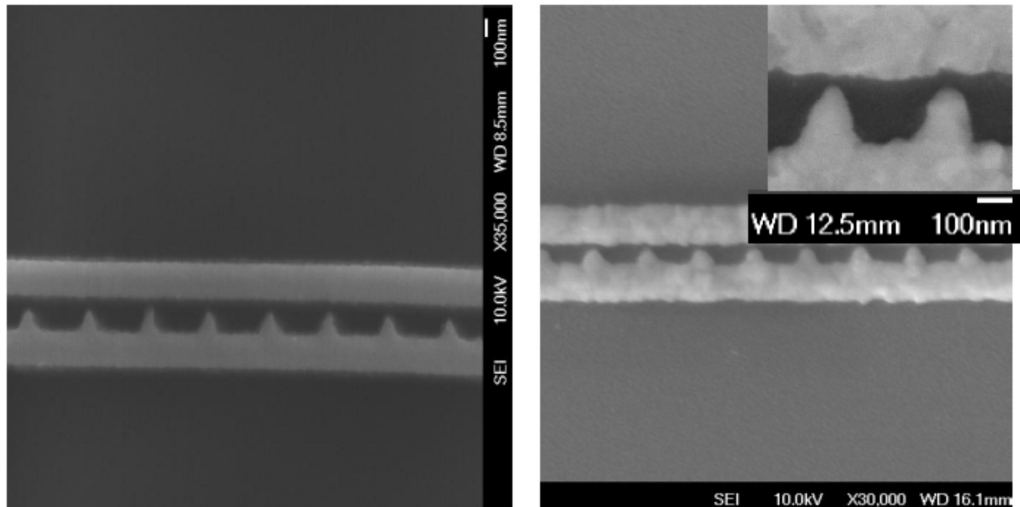


Fig. 1. **Left:** SEM image for the triangular antenna before ALD. The Tip-wall gap distance~70nm; Tip length ~100nm; Wall-wall distance~170nm. **Right:** SEM image at an intermediate stage of the ALD deposition. Tip-wall gap distance ~21nm; Tip length ~86.5nm; Wall-wall distance~108nm. Energy-dispersive X-ray spectroscopy (EDX) data after Cu ALD show that the Cu successfully grew on the Pd tips and closed the gap. Also, no growth was observed on the contact pad (A) and surrounding SiO₂ areas, as expected. The inset is a magnified view of the tips showing the selective nature of the ALD deposition.

The extension of rectennas from the microwave to the IR and visible regimes offers enormous potential benefits. In addition to the breakthroughs in our understanding of basic physics, optical rectennas would be useful in many transformative applications, including photovoltaics (the conversion of photon energy to electrical energy), solar cells (the conversion of solar energy to electrical, thermal or chemical energy), nano-photonics, near field optics, IR sensing, and imaging (including medical and chemical sensors). Another increasingly important application is the transmission and reception of information. This is significant since the density of transmitted information is greater at higher frequencies, where the density varies as the square of the frequency. Furthermore, for transmission through the atmosphere, losses decrease as the frequency increases.^{1,2}

Perhaps in direct proportion to the potential benefits, optical rectification has faced important challenges in materials processing and theoretical understanding. The device has to be optimized so that:

- The antenna is an efficient absorber of radiation encompassing the energy rich visible portion of the solar spectrum, currently not exploited fully.
- The rectifier has a response time commensurate with the range of frequencies to be rectified. For the solar spectrum, λ ranges from 10,000 to about 400 nm. In section 2, we discuss the concept of traversal time and the RC time, and discuss how the geometrically asymmetric tunnel junction (GATJ) design can be tailored to fit this requirement. This is demonstrated by a model calculation of the capacitance and corresponding RC time for a model GATJ. Moreover, as the result of recent advances in nanotechnology, Metal/Vacuum/Metal (MVM) tunnel junction gaps can now be reproducibly fabricated down to ~1 nm over cm² sized areas using selective ALD. In particular, for Cu, the selective ALD process is self-limiting at gap separations of 1 nm. This is a consequence of the chemistry and kinetics of the specific materials used in the junction. For gap distances of this size,

rectification of radiation with frequencies in the visible range is possible due to the short transit time allowing electron tunneling before field reversal.

- Impedances must be matched for efficient energy collection and conversion in rectenna devices.
- The device has a high conversion efficiency. For a simple p-n junction PV cell, the efficiency is limited by the Shockley-Quissier Limit of about 33%.^{3,4} The theoretical understanding of the operation and description of antennas at the nanoscale in the optical regime is only now being studied in a rigorous way taking into account that the behavior of metals in the optical regime differs from that at frequencies below the IR.

In this paper, we discuss the modeling, characterization, and nanofabrication of a geometrically-asymmetric rectenna device that acts as both an antenna and rectifier for IR and optical radiation. In Section 2, we review the response time of such devices, focusing on the results and implications of an important study by Nguyen et al. We also explain how tunnel junctions are capable of rectifying signals in the visible regime. In Section 3, we review the mechanisms of rectification and the experimental data confirming optical rectification, including quantum-based theoretical analyses. We also show the significance of geometry in providing both the focusing effect and the asymmetric tunneling for rectification.

2. RESPONSE TIME OF TUNNEL JUNCTIONS

In addition to the issues regarding the fabrication of reproducible nanoscale devices, the response time of the rectifying device to optical radiation is a critical element for successful operation. The response time consists of several contributions. One is the collective response of the conduction electrons that establish the AC bias. Generally for metals, the collective response corresponds to frequencies well beyond the UV (or periods of about 10^{-16} sec). Two other elements affecting device response time are the electrodynamic response of the junction to the changing fields (RC-time) and the “transversal time” for electrons to cross the gap region in the tunnel junction before field reversal. These latter two times are considered in the following subsections.

2.A. “Traversal Time” or “Tunneling Time” for Nanoscale Tunneling Junctions

The concept of “traversal time” applied to electron transmission through time-dependent barriers, is needed to estimate the limiting frequency for the tunneling rectifiers used in nanoscale devices. Qualitatively, an electron of a given energy incident on the oscillating barrier “interacts” with the barrier for a time, τ_b . Consider the two limiting cases. In one limit where the period of the oscillation, T , of the radiation is longer than this time of interaction, the electron effectively interacts with a “static” barrier and, hence, can tunnel before the field direction reverses. On the other hand for the limit where the frequency of the radiation is very high with $\tau_b \ll T$, then the electron interacts with many cycles of the radiation and the tunneling barrier is essentially unchanged due to the oscillating voltage. In this limit, the tunneling current is comprised of the photon-excited electrons which have absorbed or emitted quanta equal to $n\hbar\omega$, where $n=1,2,\dots$ and ω is the angular frequency of the incident radiation. The crossover between these two limiting behaviors may be determined by the relationship, $\omega\tau \approx 1$.⁵ The validity of such a conceptual approach has been the subject of debate and controversy ever since

the advent of quantum mechanics and the recognition that there can be particle tunneling through classically forbidden barrier regions. Basically the problem lies in the difficulty of defining and measuring the traversal time for the simple time-dependent scattering experiment in which an electron represented by a wave packet tunnels through a spatially localized barrier and is detected beyond the tunneling region.^{6,7,8}

A seminal experiment by Nguyen et al.⁹ used a dynamical approach to probe tunneling times in which a natural time scale is provided by a laser that is an integral part of the experimental arrangement. The laser incident upon an STM junction, consisting of a W-sharp tip and a polished, flat Si anode, causes the tunneling and, at the same time, provides a “clock” to measure the duration of the event. Given that the laser induced electric field is larger near the pointed apex of the tip than at the planar surface of the sample means that the vacuum tunnel barrier will tend to buckle inward (concave) or become thinner for forward bias and balloon outward (convex) or become thicker for reverse bias (see discussion and Figure 5 in Section 3.A). Moreover, if there is material asymmetry as in the Nguyen STM junction, there is an additional barrier asymmetry introduced. Such an STM junction can be a rectifier and under irradiation leads to a net DC current.

It can be argued that, if for a fixed spacing the laser frequency is too high, few electrons will be able to transfer from one electrode to the other during the half of the period when the electric field vector in the laser beam accelerates the tunneling electron. This means that one should observe a cutoff in the strength of the rectified DC signal either 1) when the frequency is increased beyond a critical value while maintaining the tip-to-surface distance s fixed or 2) when the gap width s is increased beyond a characteristic value s_c , while keeping the laser frequency constant. This latter method was used in these experiments by Nguyen, when the junction was illuminated by a 1.06- μm YAG laser. The tip-to-base gap s was then progressively increased until the laser-induced current vanished. The DC rectified current as a function of gap width for fixed frequency indicated a cutoff distance of about 2.5 nm for the 1.06 μm YAG laser line.

The Nguyen study explained such experimental results in terms of a simple model that assumes that the particle acts as if it obeys the kinematical equations of motion as the particle traverses the classically inaccessible region defining the barrier at a velocity approximately equal to the Fermi velocity. If we assume an average tunneling velocity to be the Fermi velocity, v_F , then $f_{\text{cutoff}} = v_F / s$. This analysis predicts that for a 1 nm gap with a metallic tip and vacuum barrier, the transit time of about 10^{-15} seconds corresponds to radiation approaching the UV.⁹ The technological difficulty of producing arrays of nanometer gap junctions over areas of cm^2 has recently been overcome by Gupta and Willis using selective ALD.¹⁰ Planar arrays of Cu-vacuum-Cu tunnel junctions were produced on silicon wafers using conventional lithography techniques, followed by selective ALD to yield tunnel junctions of $\sim 1\text{nm}$. This selective atomic layer deposition (ALD) process that is self-limiting at gap separations of 1 nm for Cu. At this spacing, the tunneling time is sufficiently short for electrons to transit the barrier before field reversal in the visible frequency range, leading to rectification for asymmetric barriers.

These estimates for the “traversal” time have been corroborated in a series of simulations by Mayer et al.^{11,12,13,14,15}, who have used a quantum-mechanical transfer matrix approach for the modeling of a geometrically-asymmetric, metal-vacuum-metal junction subject to an oscillating potential. This quantum mechanical scheme accounts for the three-dimensional aspects of the

problem as well as the time dependence of the barrier. The currents are obtained by solving the time-dependent Schrödinger equation with a Floquet expansion of the wave function. For simulations using a full range of frequencies in the solar spectrum, Mayer et al. investigated how the efficiency of the rectification is affected by the aspect ratio of the tip, the work function of the metallic elements and the occurrence of polarization resonances. Their results demonstrate that the rectification of infrared and optical radiation is possible using devices of the type proposed by the authors.

2.B. RC-Time for Geometrically-Asymmetric Tunneling Junction (GATJ) Rectifiers

For the case of a planar MIM structure, the RC response-time of the junction is limited by parasitic capacitance yielding a practical limit of 10-100 THz.¹⁶ By contrast, point-contact devices (i.e., whisker diodes, and GATJs whose geometry is essentially the same) have been used in measurements of absolute frequencies up to the green part of the visible spectrum, demonstrating a response time of the order of femtoseconds, orders of magnitude faster than conventional MIM diodes.¹⁷ The asymmetrical, non-planar geometry of the pointed whisker in conjunction with the flat anode is an essential requirement for increasing the cutoff frequency ω_c of the diode, but inconsistent with the planar geometry of MIM tunneling theory for which the cutoff frequency is independent of contact area. In earlier studies of the detection and harmonic generation in the submillimeter wavelength region, Dees¹⁸ emphasized the importance of using the point-contact geometry to reduce the shunting effect of the capacitance and thus increase the high frequency cutoff of the device. Indeed the response time $\tau = 1/\omega_c = RC$ is independent of contact area for a planar MIM geometry since C, the capacitance of the contact, is proportional to A, the contact area, whereas R the resistance is inversely proportional to A. On the other hand, for a point contact geometry, it can be shown using a solvable model with a spherical tip that ω_c is no longer independent of the tip radius (or area), and the sharper the tip, the faster the response time of the diode.^{16,19} Although mechanical stability of these earlier devices placed a limitation on producing robust sharp tips, modern fabrication techniques have overcome the mechanical fragility of previous point contact diodes and issues related to reproducible fabrication of nanoscale devices.

Below we provide a more detailed discussion of why it is necessary to use GATJs with sharp tips to obtain RC times short enough for rectifying radiation at high frequencies.

Such models are important for understanding individual device operation and final integration of devices into complex circuits. These device-circuit equivalents, such as that for a tunneling diode, allow for the direct application of the Kirchhoff Current and Voltage Laws which are, in turn, applications of conservation of charge and energy. In determining the equivalent device model, resistances (R), capacitances (C) and inductances (L) are used either as lumped (wavelength independent) or distributed (wavelength dependent, transmission line, R,L,C per unit length) elements.

For the case of the rectenna with a GATJ rectifier, a lumped circuit model consists of a resistance for the metallic antenna taking into account its geometric properties (i.e., the tip that is part of the GATJ) while the junction is modeled as a capacitance with a large shunt resistance. This junction corresponds to the traditional modeling of a low leakage capacitor. Such a junction and resistive line feeding element represent a single time constant circuit as illustrated in Fig. 3. It can be shown that this transient circuit has a time constant τ given by:

$$\tau = RC \left(\frac{R_s}{R + R_s} \right) \quad (1)$$

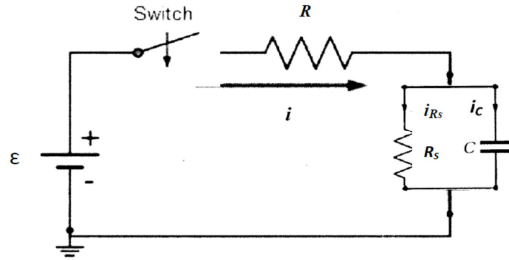


Fig. 3. Equivalent circuit model of a rectenna with metallic antenna resistance R and junction capacitance C in parallel with junction shunt resistance R_s

The lumped circuit element R in Fig. 3 includes implicitly the geometrical nature of the circuit elements. It should be noted that except for the pointed antenna tip coupled to the junction anode (not vacuum), the quantities R^{-1} , C , and R_s^{-1} are all proportional to A . However, for an antenna modeled as a spherical tip, the antenna resistance R is proportional to r_s^{-1} , the inverse of radius of curvature of the tip. Hence, the response time RC is proportional to r_s or $A^{1/2}$. The smaller the tip radius, the shorter the response time.

Alternatively we can consider the same circuit but analyze its steady-state behavior under an ac signal rather than under transient conditions.¹⁹ Following Sullivan et al.¹⁹, we now define ω_c as the frequency at which half the power is dissipated in the series resistance R . For this traditional half-maximum power limit for operation, the result is:

$$R = \frac{R_s}{1 + \omega_c^2 C^2 R_s^2} \quad (2)$$

For $\omega_c^2 C^2 R_s^2 \gg 1$, this leads to the following condition for ω_c ,

$$\omega_c^2 C^2 R_s R = 1 \quad (3)$$

We now demonstrate that ω_c is proportional to $r_s^{-1/2}$. The quantity C is proportional to A , R_s is proportional to A , and R is inversely proportional to r_s ; hence,

$$\omega_c = \sqrt{\frac{1}{R_s R C^2}} \propto \sqrt{\frac{1}{(1/\pi r_s^2) r_s^{-1} (\pi r_s^2)^2}} \propto r_s^{-1/2} \quad (4)$$

As the tip radius decreases the cutoff frequency increases. This reasoning led to the use of “ultra-fine” tips in the absolute frequency measurements of Javan and collaborators²⁰ in which a thin, Tungsten wire several microns in diameter and approximate length of 1 mm was mounted at the end of a coaxial cable. The tip of the W wire was sharpened by means of a standard etching technique to a diameter of less than 100 nm.

Although neither the transient nor ac circuit approaches truly represent the GATJ but represent reasonable models for the rectifier, these approaches indicate that the RC response of the GATJ depends on the radius of curvature of the tip or contact area. The RC time constant has a dependence ranging between being proportional to r_s and $r_s^{1/2}$, thus predicting that sharp tips used in the GATJ rectifier can be used to produce devices that can rectify radiation in the visible region.

As an example, we estimate the RC time constant of a rectenna with a GATJ (coupled to the anode) device with geometric parameters associated with one of our prototype devices similar to the one illustrated in Fig. 1. We consider a typical periodic unit cell of this device, with a single nanoantenna. The prototype device consists of ten thousand unit cells, placed in parallel. For this first-order estimation of the RC time constant, we use material parameters that correspond to the limit when $\omega \rightarrow 0$. It is understood that frequency-dependent parameters should be used when considering frequencies in the visible, in particular for frequencies at which polarization resonances occur. The experimental device is essentially a two-dimensional flat structure. The periodic unit cell in our modeling has a length $L_x = 350 \text{ nm}$ along the x -axis and a cathode-anode spacing $L_y = 295 \text{ nm}$ along y . A value of 100 nm is taken for the thickness W of the structure. We represent the antenna by a flat triangle whose apex is replaced by a half-circular disc of radius r_{apex} that connects smoothly to the sides of the triangle. Initially, before the ALD metallization, the antenna has a base $B = 110 \text{ nm}$, a height $H = 245 \text{ nm}$ and a radius of curvature $r_{\text{apex}} = 16 \text{ nm}$. The gap spacing between the apex of the antenna and the anode is 50 nm. The Ohmic resistance is estimated from a simple model in which we represent the antenna by the succession of slabs. For Cu, we obtain an Ohmic resistance $R = 0.737 \Omega$.

In order to determine the geometric capacitance C of a unit cell of the device, we calculate numerically the electrostatic energy $CV^2/2$, under a static voltage V_{ac} between the cathode and the anode. The electric potential in the unit cell of the device is obtained by solving Laplace’s equation $\nabla(e\nabla V) = 0$ (this expression is relevant to the static limit in which $\omega \rightarrow 0$ and the antenna is assumed to have a dielectric constant $\varepsilon \rightarrow -\infty$). The resolution of Laplace’s equation is achieved by using a finite-difference technique.²¹ This resolution provides the electric potential $V(r)$ in the system from which we can compute the electric field, $E = -\nabla V$. The geometrical capacitance C of the system considered is finally obtained from the relation

$$\frac{1}{2}CV^2 = \iiint_{\text{unit_cell}} \frac{1}{2} \varepsilon |E|^2 dv \quad (5)$$

in which the right-hand side provides the electrostatic energy one must provide to a unit cell of the device in order to establish V_{ac} . For the system represented in Fig. 14, we obtain a geometric capacitance $C = 2.94 \times 10^{-18} \text{ F}$ and a resulting RC time constant of $2.2 \times 10^{-18} \text{ s}$, a value corresponding to frequencies beyond the visible.

We can study how the parameters R , C and $\tau = RC$ are modified by a conformal two-dimensional expansion of the antenna. A series of antennas are generated for which the parameters B , H and r_{apex} used for Fig. 3 are multiplied by a common dilatation factor α where α ranges from 1 to 1.204. In this expansion, the height H of the antennas increases progressively from 245 nm to 294 nm, so that the gap spacing between the apex of the antenna and the anode is reduced progressively from 50 nm to 1 nm. The base B of then increases at the same time from 110 nm to 132.45 nm. The parameters L_x , L_y and W of the device are kept constant. The Ohmic resistance R of the antenna remains approximately constant. The geometric capacitance C ranges from $2.94 \times 10^{-18} \text{ F}$ (for $H = 245 \text{ nm}$) to $1.69 \times 10^{-17} \text{ F}$ (for $H = 294 \text{ nm}$) and the RC time constant increases from $2.2 \times 10^{-18} \text{ s}$ to $1.2 \times 10^{-17} \text{ s}$, respectively. This dependence of the capacitance C as H increases from 245 nm to 294 nm is represented in Fig. 4.

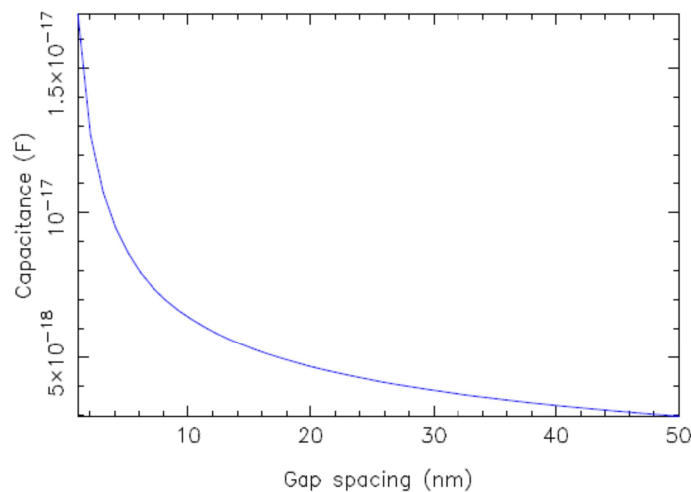


FIG. 4. Capacitance C of a unit cell of the device, when the antenna is affected by a conformal planar expansion with the dilation parameter goes from 1 to 1.204. The results are represented as a function of the gap spacing d between the apex of the antenna and the anode, as H increases from 245 nm to 294 nm and the radius of curvature increases from 16 nm to 19.3 nm. The Ohmic resistance R of the antennas including the sharp tip is calculated to be 0.737Ω .

From the simulations, the RC time constant of the device structures in this work should not be a limiting factor for applications related to the rectification of optical radiation, where the static values of the parameters are applicable. The extension of these simulations taking into account the frequency dependence of the material parameters is currently under investigation.

3. RECTIFICATION IN TUNNEL JUNCTIONS

3.A. Mechanisms for Rectification in Tunnel Junctions

The I-V characteristics of a tunneling junction are determined by 1) the flux of electrons in given initial states incident on the barrier interface and their occupation probabilities that depend on temperature and field, 2) the available final states and their occupation probabilities, and 3) the shape of the tunnel barrier, which may be modified due to contact potentials, surface photovoltage effects, induced AC voltages due to laser irradiation, etc. Correspondingly, the

current asymmetry (or rectification properties) at fixed gap width s must originate from one or several possible causes discussed below, namely material, geometrical, thermal asymmetry, and photo-stimulated changes in the electron flux distribution.^{22,23,24} We describe here the geometric asymmetry of the rectenna due to the modification of the field distribution in device that is the critical element for achieving high frequency rectification.

3.A. Rectification due to Barrier Modification by Asymmetric Geometry

For nanometer gap distances, the nature of the tunneling phenomenon is such that the current passes predominantly through that sharp protrusion closest to the planar sample surface. In such conditions and even in the absence of any material asymmetry (e.g., W tip, W surface, and assuming no work function inhomogeneities), the shape of the tunnel barrier is asymmetric as a function of the applied bias field. This is due to the geometric asymmetry of the electrodes comprising the tunnel junctions. This effect is illustrated in Fig. 5.

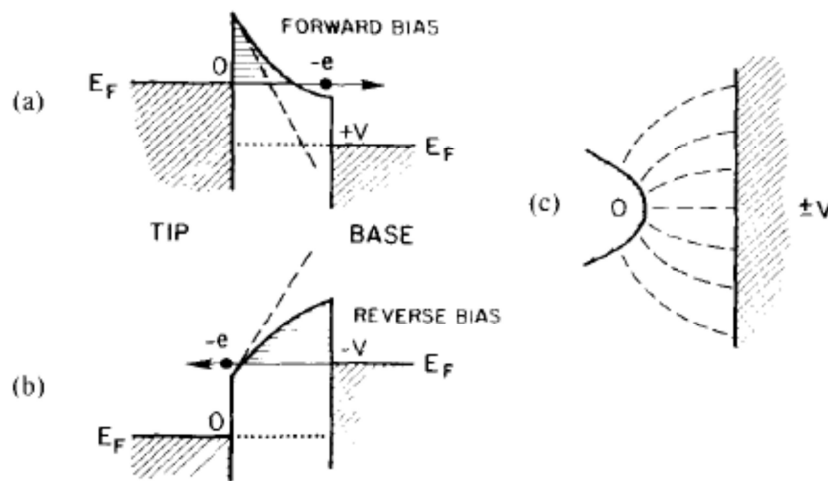


Fig. 5. (c) A tunnel barrier of a materially-symmetric, geometrically-asymmetric junction. The barrier exhibits a concave shape for (a) forward bias and (b) convex shape for reverse bias.⁹

It is evident that the static electric field gradient is larger near the pointed apex of the tip than at the planar surface of the sample. This means that the vacuum tunnel barrier will tend to buckle inward or become thinner for forward bias and balloon outward or become thicker for reverse bias. The first observation of the geometrical asymmetry effect in a STM was observed by Feenstra et al.²⁵ and in the detailed study of rectification in an STM presented by Nguyen et al.⁹ In addition, Dagenais et al.²⁶ have experimentally verified that a geometrically asymmetric tunneling diode can be used to rectify radiation through the RF region. Based on their experiments, they envision that higher conversion efficiencies will be achieved at mid IR frequencies. Most recently, Ward et al.²⁷ have shown both experimentally and theoretically that nonlinear tunneling conduction between gold electrodes separated by a subnanometer gap leads to optical rectification, producing a DC photocurrent when the gap is irradiated by a 785 nm laser source. In a recent paper, the authors have reviewed experiments verifying the geometrical rectification mechanism.²⁸ Extensive simulations studies of geometrically asymmetric tunnel junctions verify these observations. In particular, the work of Mayer et al. provides insight into the development and optimization of devices that could be used for the efficient energy conversion of infrared and optical radiations. The studies also demonstrate that an accurate

treatment of nanoscale tunnel junctions operating in the near IR and visible requires a quantum-mechanical treatment.¹¹⁻¹⁵

3.B. Experiments Verifying Rectification Mechanisms from the Microwave through the Visible Region—Geometrical Effects

In this section we review some of the experiments verifying that an STM and other nanojunctions structures can act as antennas and rectifying devices for electromagnetic radiation from the microwave through the visible.

In a series of experiments, Kuk et al.^{29,30} used an STM consisting of a metal tip (Au) and a semiconductor sample anode (e.g., Si), which was illuminated with laser radiation below and above the semiconductor indirect band gaps, specifically, photon energies of 2.94 eV, 1.96 eV, 1.17 eV, and 0.95 eV. The STMs were modified using a small lens to focus the laser beam to near its diffraction limit, yielding power densities up to 5.0 kW/cm^2 on the junction.³¹ The resulting induced bias was measured laterally along the surface as light-induced excess current and voltage. For photon energies exceeding the band gap energy, surface photovoltages (SPV) of about 300 mV were induced across the gap independent of illumination intensity and frequency. For a photon energy of 0.95 eV, no surface photovoltage was detected. A small, atomically scaled (laterally along the surface) varying dc signal of 3 to 5 mV was also observed in the experiments. The authors suggest that this small signal is due to optical rectification associated with the geometric asymmetry of the junction. These striking results using a Au tip and collector demonstrate that the STM junction can absorb and rectify radiation corresponding to wavelengths shorter than $1.06 \mu\text{m}$ in agreement with the experimental results of Nguyen et al.⁹

Tu et al.³² have experimentally verified that an STM junction can rectify radiation in the microwave region, which has led to the first direct, quantitative measurement of the rectification current due to single atoms and molecules. In their work, microwave of known amplitude and frequency irradiated the junction of a low temperature scanning tunneling microscope producing an electric field between the tip and an atom or molecule on the anode surface. It induced a DC signal that is spatially localized and exhibits chemical sensitivity at the atomic scale.

In 1998, Bragas et al.,³³ used a laser with wavelength of 670 nm to irradiate an STM junction to determine the field enhancement as measured by optical rectification. A field enhancement factor between 1000 and 2000 was obtained for highly oriented pyrolytic graphite and between 300 and 600 for gold. Analysis of their data indicated optical rectification due to junction geometry as well as thermal asymmetry. The admittance of $\partial^2 I_{stat} / \partial V_{stat}^2 \big|_{V_{dc}}$ was determined to be significant only for p-polarized light and in phase with the intensity variation, consistent with the expected behavior for the rectified current. Their experiments indicate that visible light (640 nm) can be rectified using nm-sized tunnel junction devices.

Most recently, Ward et al. have shown both experimentally and theoretically that “nonlinear tunneling conduction” between gold electrodes separated by a subnanometer gap leads to optical rectification when the gap is irradiated by a 785 nm laser source, producing a DC current.²⁷

3.C. Simulation Studies of Geometrically Asymmetric Tunnel Junctions

Unlike a conventional planar MIM or MVM diodes, devices employing a pointed nanowire tip achieve rectification solely or primarily with geometrical asymmetry.^{34,35} This is illustrated in Fig. 6 where the rectification ratio of a W-W junction (no material asymmetry) is compared using planar and pointed geometries. Figure 6 shows clearly that a planar geometry (with $r \rightarrow \infty$) provides no rectification, i.e., a rectification ratio (forward current divided by reverse current) of one.³⁴

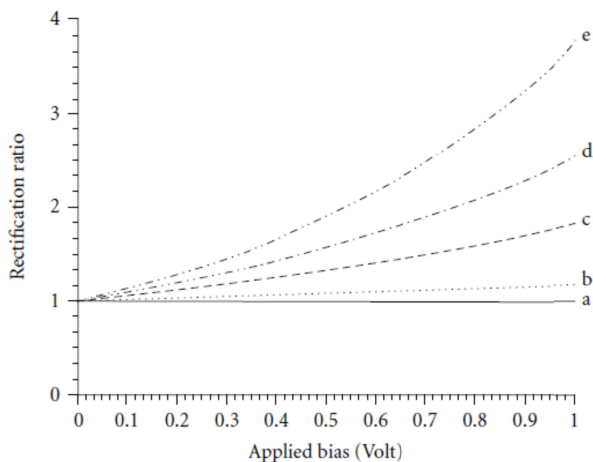


Fig. 6. Effect of tip radius, r , on the rectification ratio. The calculations were done for (a) $r \rightarrow \infty$, planar-planar junction; (b) $r = 10 \text{ nm}$; (c) $r = 2 \text{ nm}$; (d) $r = 1 \text{ nm}$; and (e) $r = 0.5 \text{ nm}$, all for a separation of 2 nm .³⁴

Early theoretical work on the tunneling characteristics of these junctions usually relied on approximations in the shape of the barrier and in the tunneling probabilities, which were typically based on a one-dimensional model.^{6,36} However, modern computational facilities make it possible to address this problem more rigorously using quantum-mechanical techniques including three-dimensional aspects of the detailed atomic structure and the tunneling barrier. Such studies make it possible to investigate the geometric, material, and operational parameters that are important in optimizing the performance of geometrically-asymmetric devices.

Lucas et al.³⁷ used a formulation of elastic, one-electron tunneling through three-dimensional, non-separable, spatially-localized barriers within the context of potential-scattering theory. They applied this approach to a model metal-vacuum-metal junction, consisting of two parallel electrodes, one of which containing a hemispherical protrusion. The electronic structure of each metal electrode is assumed to be free-electron-like. They found that the current distribution peaks within a narrow angle around the boss axis, confirming earlier estimates based on transfer-Hamiltonian formalism and in agreement with the observed atomic resolution of an STM microscope, when operating with atomic-size tips.

A theoretical study by N. D. Lang, A. Yacoby and Y. Imry in 1989 on a single-atom point source of electrons indicates that the current from a field-emission tip terminated by a single atom yield a relatively focused, high-current beam with a narrow energy distribution, in agreement with experimental studies.³⁸ The results are physically interpreted in terms of channel filtering by an adiabatic constriction. This is a consequence of the potential distribution due to the particular geometry,

Mayer et al.¹¹ presented a transfer-matrix analysis of a GATJ with a flat anode and a cathode with a hemispherical protrusion. This work confirmed the conclusions of Lucas et al.³⁴ and explored how the rectification properties of such systems depend on their physical and geometrical parameters. This analysis still relied on a quasi-static approximation, in which it is assumed that one can compare currents obtained for static values of the external bias. This approximation is valid in the far-infrared ($\omega \rightarrow 0$) but must be replaced by a more exact approach in order to treat situations in which the time that electrons take to cross the junction is comparable with the period of the oscillating barrier.

In a subsequent paper Mayer et al.¹² extended their previous work by taking into account the time dependence of the external bias explicitly using the transfer-matrix approach and the time dependent Schrödinger Equation. They assume that the geometrically asymmetric tunnel junction consisted of a cathode metal supporting a hemispherical protrusion with a height of 1 nm, a radius of 0.5 nm, and separation between the apex of the tip and the planar electrode of 1 nm. Due to the external electromagnetic radiation of varying frequency and intensity, there is an impressed oscillating potential across the junction, $V(t) = V_{ac} \cos(\omega t)$. In the simulations, V_{ac} varies from 0.01V to 1.0V and frequencies that correspond to quanta of energy between 0.2 eV ($\lambda = 6200 \text{ nm}$) in the IR and 5eV ($\lambda = 248 \text{ nm}$) in the UV. The rectification ratio that one obtains by taking the ratio of the mean values of the forward, I^+ , and reverse, I^- , currents is plotted in Fig. 7. The values obtained at low frequency, $\omega \rightarrow 0$, agree with those obtained in the quasi-static analysis.¹¹ Because of the photon-absorption processes, the rectification ratio, R , first increases with ω before decreasing at higher frequencies. The intermediate region proves that the rectification of optical frequencies can be achieved by the device, which agrees with conclusions reached earlier by Sullivan, et al.¹⁶ In a quasi-static analysis, they predict a cutoff of the rectification for a photon-energy around 4 eV (radiation with wavelength of 300 nm in ultraviolet) because the field would then reverse before the electrons can cross the junction. Indeed, this oscillating-barrier analysis shows a significant decrease in rectification at that frequency.

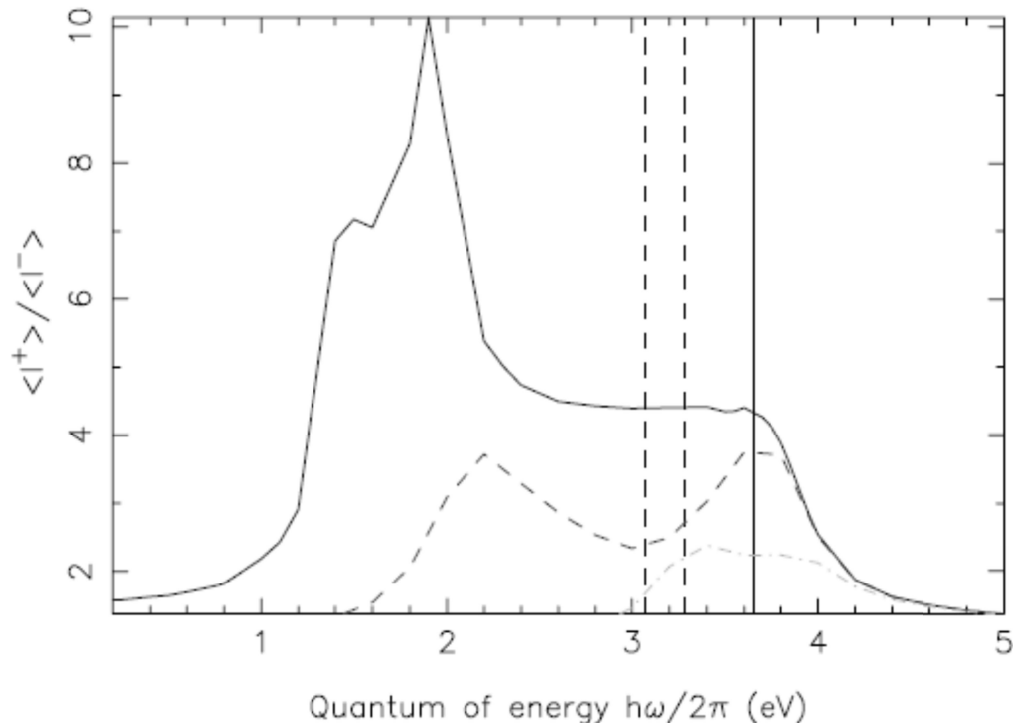


Fig. 7. Rectification ratio as obtained for a geometrically asymmetric junction subject to an external bias $V_{ac} \cos(\omega t)$ with $V_{ac} = 1$ (solid line), 0.1 (dashed) and 0.01 V (dot-dashed line). The quantum of energy $\hbar\omega$ ranges between 0.2 and 5 eV. The vertical lines indicate the height of the surface barrier (as measured from the Fermi level of the emitting metal) when V_{ac} (dashed line, left), -1 (dashed line, right), and 0 V (solid line).¹²

In order to assess the importance of the deposition of noble metals, known to have plasmonic resonances, on the field enhancement and rectification properties of a model tunneling junction, Mayer et al. performed 3D quantum mechanical computer simulations of optically irradiated MVM tunnel junctions using Ag and W tips.¹³ They predict an enhanced rectification and current output due to the surface plasmonic resonances in Ag at ~ 3 eV, corresponding to the energetic green portion of the visible spectrum. This study also explained the role of these plasmons and more generally of the frequency-dependence of the dielectric function on the rectification properties of the junction. In Fig. 8, we plot the results of their simulations. Compared to tungsten, the power gained by the electrons that cross the device, and the rectification ratio of the device are enhanced by several orders of magnitude at frequencies that correspond to a resonant polarization of the tip.

These results suggest that the dependence of the plasmon frequencies on both the material and the geometry of the tip could be used to control the frequency at which the junction is the most efficient for the rectification of external signals. It is also important to note that there is a significant contribution of multi-photon processes (especially for $\hbar\omega \approx |eV_{ac}|$), which is most pronounced when a polarization resonance occurs. This effect opens the possibility to build devices for the selective detection of radiation in the infrared or visible domain or for a more efficient rectification and conversion of their energy. It is expected that deposition of a thin layer

of other noble metals on an underlying antenna structure such as tungsten, molybdenum or aluminum should yield similar results.

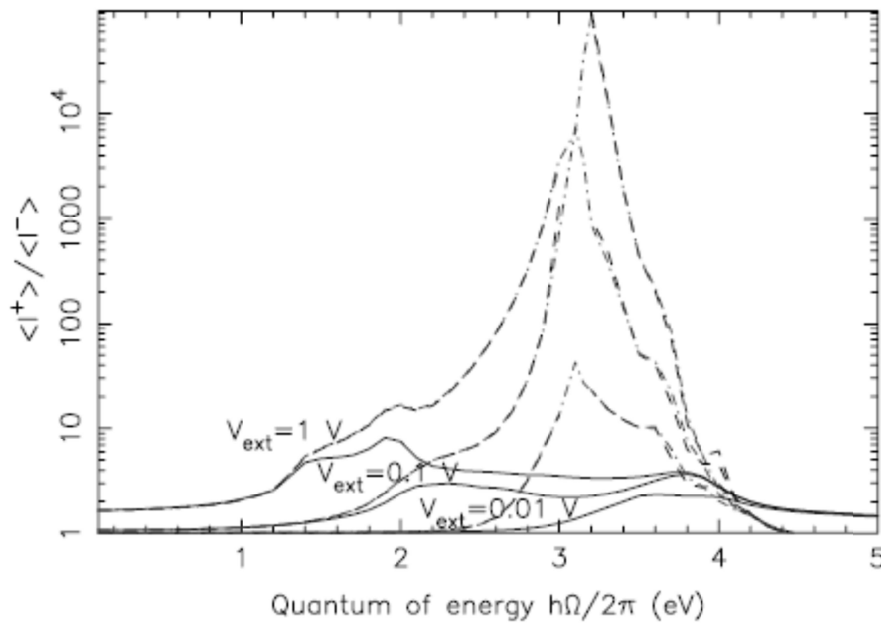


Fig. 8. Rectification ratio of a junction made of silver and subject to an external bias $V_{ac} \cos(\omega t)$, with $V_{ac} = 1, 0.1$ and 0.01 V. The solid, dashed and dot-dashed lines indicate results using $\varepsilon(\omega) \rightarrow -\infty$, $\varepsilon(\omega) = 1 - \omega_p^2 / \omega^2$, and $\varepsilon(\omega) = 1 - \omega_p^2 / (\omega^2 + i\omega / \tau)$, respectively, as models for the dielectric function of the tip. Results obtained at the 3.1 eV resonance energy with $\varepsilon(\omega) = 1 - \omega_p^2 / \omega^2$ are off-scale and not shown.¹³

Mayer et al. also observed a significant enhancement of the energy conversion at frequencies that correspond to a resonant polarization of the tip.¹⁴ The dependence of these resonance frequencies on the shape and on the material used for the tip therefore gives the possibility of controlling the frequency at which the device is most efficient for the rectification of external radiation. It also was shown that reducing the work function of the metallic elements increases the performance. For practical applications, one may consider two-dimensional arrays in which devices would be placed with a typical spacing of $10 \mu\text{m}$ between adjacent protrusions. The currents and energies achieved per square meter correspond in this case to those achieved for a single tip times a typical factor of 10^{10} . These results demonstrate that the rectification of radiation with typical frequencies in the infrared and optical domains can be achieved by using geometrically asymmetric, metal–vacuum–metal junctions. The results also provide a more quantitative analysis of the efficiency with which the energy of incident radiation can be converted by such devices.

The work of Mayer et al. provides insight into the development and optimization of devices that could be used for the efficient energy conversion of infrared and optical radiations. The studies also demonstrate that an accurate treatment of nanoscale tunnel junctions operating in the near IR and visible requires a quantum-mechanical treatment.^{11–15}

5. SUMMARY

We have surveyed developments related to the fabrication and theoretical understanding of our proposed nanoscale rectennas. These rectenna devices, based on the geometrically-asymmetric tunnel junction, can collect and rectify electromagnetic radiation, from the infrared through the visible regimes. Studies of electron transversal time and RC response time demonstrate that tunnel junctions formed with a sharp tip (early examples of which are the whisker diode and the STM probe) are capable of operating into the UV regime. Recent efforts to construct nanoscale antennas reveal a wealth of promising geometries and fabrication techniques. Other recent experimental work confirms that nanorectennas are capable of not just receiving, but also rectifying, signals through the visible regime. A number of past and recent ongoing simulation studies not only demonstrate the viability of the geometrically-asymmetric tunnel junction, but also establish the importance of certain design parameters (choice of geometry and materials) that will be crucial in efforts to optimize such devices.

Acknowledgements

We thank Dr. Moon S. Chung (Ulsan University, Ulsan, S. Korea) and Dr. A. A. Lucas (Universitaires Notre-Dame de la Paix, Namur, Belgium) for their useful reviews and critiques. We also acknowledge the assistance of and useful discussions with William Mansfield, former Director of Operations of the Nanofabrication Laboratory at The Pennsylvania State University, and his associates at the facility. This work was supported in part under NSF Grant No. 1231313, Division of Electrical, Communications and Cyber Systems, under the Program: Energy, Power, Adaptive Systems-EPAS.

- ¹ J. Alda, J. Rico-García, J. López-Alonso, and G. Boreman, "Optical antennas for nano-photonics applications," *Nanotech.* **16**, S230 (2005).
- ² Palash Bharadwaj, Bradley Deutsch, and Lukas Novotny, "Optical Antennas," *Adv. Opt. and Photonics* **1**, 438 (2009).
- ³ P. B. Lerner, N. M. Miskovsky, P. H. Cutler, A. Mayer, and Moon S. Chung, "Thermodynamic Analysis of High Frequency Rectifying Devices: Determination of the Efficiency and Other Performance Parameters," *Nano Energy*, Volume 2, Issue 3, 368–376 (2013).
- ⁴ Saamil Joshi and Garret Moddel, "Efficiency limits of rectenna solar cells: Theory of broadband photon-assisted tunneling," *Appl. Phys. Lett.* **102**, 083901 (2013).
- ⁵ M. Büttiker and R. Landauer, "Traversal Time for Tunneling," *Phys. Rev. Lett.* **49**, 1739 (1962).
- ⁶ C. B. Duke, *Tunneling in Solids*, New York, Academic, 1969.
- ⁷ P. H. Cutler, T. E. Feuchtwang, T. T. Tsong, Y. Kuk, H. Nguyen, and A. A. Lucas, "Proposed use of a scanning-tunneling-microscope tunnel junction for the measurement of tunneling time," *Phys. Rev.* **B 35**, 7774 (1987).
- ⁸ L. V. Keldysh, "Ionization in the Field of a Strong Electromagnetic Wave," *J. Exptl. Theoret. Phys. (USSR)* **47** (1964) 1945-1957, translation: *Soviet Physics JETP* **20** (1965) 1307-1314. Keldysh presented another, not altogether incompatible, criterion for adiabatic transmission through the oscillating barrier. The crossover between the multiphoton absorption and the quasi-static tunneling is determined by the Keldysh parameter $\gamma_K = \omega(2m_e V_b / e^2 E^2)^{1/2}$, where m_e is the electron mass, e the charge on the electron, E is the electric field strength generated by the laser and ω is the angular frequency of the radiation. In the case of a metal, the height of the barrier, V_b , is typically identified with the work function and for a semiconductor with the band gap. As would be expected a value of $\gamma_K \gg 1$ indicates multiphoton processes dominate (in the barrier and/or tunneling process), and, $\gamma_K \ll 1$ implies tunneling processes dominate.
- ⁹ H. Q. Nguyen, P. H. Cutler, T. E. Feuchtwang, Z-H. Huang, Y. Kuk, P. J. Silverman, A. A. Lucas, and T. E. Sullivan, "Mechanisms of Current Rectification in an STM Tunnel Junction and the Measurement of an Operational Tunneling Time," *IEEE Trans. Elec. Dev.* **36**, 2671 (1989).
- ¹⁰ R. Gupta and B.G. Willis, "Nanometer spaced electrodes using selective area atomic layer deposition," *Appl. Phys Lett.* **90**, 253102 (2007).
- ¹¹ A. Mayer, M.S. Chung, B.L. Weiss, N.M. Miskovsky and P.H. Cutler, "Three-dimensional analysis of the geometrical rectifying properties of metal-vacuum-metal junctions and extension for energy conversion," *Phys. Rev. B* **77**, 085411 (2008).
- ¹² A. Mayer, M.S. Chung, B.L. Weiss, N.M. Miskovsky, P.H. Cutler, "Three-dimensional analysis of the rectifying properties of geometrically asymmetric metal-vacuum-metal junctions treated as an oscillating barrier," *Phys. Rev. B* **78**, 205404 (2008).
- ¹³ A. Mayer and P.H. Cutler, "Rectification properties of geometrically asymmetric metal-vacuum-metal junctions: a comparison between tungsten and silver tips to determine the effects of polarization resonances," *J. Phys. Condens. Mat.* **21**, 395304 (2009).
- ¹⁴ A. Mayer, M.S. Chung, B. L. Weiss, N. M. Miskovsky and P. H. Cutler, "Simulations of infrared and optical rectification by geometrically asymmetric metal-vacuum-metal junctions for applications in energy conversion devices," *Nanotech.* **21**, 145204 (2010).
- ¹⁵ A. Mayer, M.S. Chung, P.B. Lerner, B.L. Weiss, N.M. Miskovsky and P.H. Cutler, "Classical and quantum responsivities of geometrically asymmetric metal-vacuum-metal junctions used for the rectification of infrared and optical radiations," *J. Vac. Sci. Tech. B* **29**, 041802 (2011); A. Mayer, M.S. Chung, P.B. Lerner, B.L. Weiss, N.M. Miskovsky and P.H. Cutler, "An analysis of the efficiency with which geometrically asymmetric metal-vacuum-metal junctions can be used for the rectification of infrared and optical radiations," *J. Vac. Sci. Technol. B* **30**, 031802 (2012).
- ¹⁶ T. Sullivan, Young Kuk, and P. H. Cutler, "Proposed Planar Scanning Tunneling Microscope Diode: Application as an Infrared and Optical Detector," *IEEE Trans. on Electron. Dev.* **36**, 2659 (1989).

- ¹⁷ K. M. Evenson, "Frequency measurements from the microwave to the visible, the speed of light, and the redefinition of the meter," in *Quantum Metrology and Fundamental Physical Constants*, P. H. Cutler and A. A. Lucas, Eds. New York: Plenum, 1983.
- ¹⁸ J. W. Dees, "Detection and Harmonic Generation in the Submillimeter Wavelength Region," *Microwave Journal* **9**, 48 (1966).
- ¹⁹ T. E. Sullivan, Ph. D. thesis (1977), "Thermal and field emission effects of laser radiation on metal whisker diodes: Application to infrared detection devices," available from UMI (University Microfilms International), now called Bell and Howell Information and Learning.
- ²⁰ A. Sanchez, S.K. Singh, A. Javan, "Generation of infrared radiation in a metal-to-metal point-contact diode at synthesized frequencies of incident fields: a high speed broad-band light modulator," *Appl. Phys. Lett.* **21**, 240 (1972).
- ²¹ A. Mayer and Ph. Lambin, "Calculation of the electrostatic forces that act on carbon nanotubes placed in the vicinity of metallic protrusions," *Nanotech.* **16**, 2685 (2005).
- ²² N.M. Miskovsky, S. J. Shepherd, P. H. Cutler, T. E. Sullivan, and A. A. Lucas, "The importance of geometry, field, and temperature in tunneling and rectification behavior of point contact junctions of identical metals," *Appl. Phys. Lett.* **35**, 560 (1979).
- ²³ N. M. Miskovsky, P. H. Cutler, T. E. Feuchtwang, S. J. Shepherd, A. A. Lucas, and T. E. Sullivan, "Effect of geometry and multiple-image interactions on tunneling and I-V characteristics of metal-vacuum-metal point contact junctions," *Appl. Phys. Lett.* **37**, 189 (1980).
- ²⁴ Stefan Grafström, "Photoassisted scanning tunneling microscopy," *J. Appl. Phys.* **91**, 1717 (2002), and references therein.
- ²⁵ R. M. Feenstra, J. A. Stroscio, and A. P. Fein, "Tunneling spectroscopy of the Si(111) 2 x 1₁ surface," *Surf. Sci.* **181**, 295 (1987).
- ²⁶ M. Dagenais, K. Choi, F. Yesikoy, A. N. Chryssis, M. C. Peckerar, "Solar Spectrum Rectification Using Nano-Antennas and Tunneling Diodes," *Proc. SPIE*, Vol. 7605, 76050E-1 (2010).
- ²⁷ Daniel R. Ward, Falco Hüser, Fabian Pauly, Juan Carlos Cuevas and Douglas Natelson, "Optical rectification and field enhancement in a photonic nanogap," *Nat. Nanotechnol. Lett.* **5**, 732 (2010).
- ²⁸ Nicholas M. Miskovsky, Paul H. Cutler, A. Mayer, Brock L. Weiss, Brian Willis, Thomas E. Sullivan, and Peter B. Lerner, "Nanoscale Devices For Rectification Of High Frequency Radiation From The Infrared Through The Visible: A New Approach," *Journal of Nanotechnology* (2012).
- ²⁹ Y. Kuk, R. S. Becker, P. J. Silverman, and G. P. Kochanski, "Optical Interactions in the Junction of a Scanning Tunneling Microscope," *Phys. Rev. Lett.* **65**, 456 (1990).
- ³⁰ Y. Kuk, R. S. Becker, P. J. Silverman, and G. P. Kochanski, "Photovoltage on silicon surfaces measured by scanning tunneling microscopy," *J. Vac. Sci. Technol. B* **9**, 545 (1991).
- ³¹ In comparison, an estimate of the power density for a laser with a power output of 20mW and a beam diameter of about 300 μm is on the order of 20 W/cm².
- ³² X. W. Tu, J. H. Lee, and W. Ho, "Atomic-scale rectification at microwave frequency," *J. Chem Phys.* **124**, 021105 (2006).
- ³³ A. V. Bragas, S. M. Landi, and O. E. Martinez, "Laser field enhancement at the scanning tunneling microscope junction measure by optical rectification," *Appl. Phys. Lett.* **72**, 2075 (1998).
- ³⁴ A. A. Lucas, A. Moussiaux, M Schmeits, and P. H. Cutler, "Geometrical asymmetry effects on tunneling properties of point contact junctions," *Commun. Phys.* **2**, 169 (1977).
- ³⁵ Bo Lee, E. F. Barasch, T. Mazumdar, P. M. McIntyre, Y. Pang, H. J. Trost, "Development of knife-edge field emission cathodes on (110) silicon wafers," *Appl. Surf. Sci.* **67**, 66 (1993).
- ³⁶ P. H. Cutler, Jun He, J. Miller, N.M. Miskovsky, B. Weiss, and T.E. Sullivan, "Theory of Electron Emission in High Fields from Atomically Sharp Emitters: Validity of the Fowler-Nordheim Equation," *Prog. In Surf. Sci.* vol. 42, 169 (1993).
- ³⁷ A. A. Lucas, H. Morawitz, and G. R. Henry, J.-P. Vigneron, Ph. Lambin, P. H. Cutler and T. E. Feuchtwang, "Scattering-theoretic approach to elastic one-electron tunneling through localized barriers: Application to scanning tunneling microscopy," *Phys. Rev. B* **37**, 10708 (1988).
- ³⁸ N.D. Lang, A. Jacoby, and Y. Imry, "Single-Atom Point Source for Electrons," *Phys. Rev. Lett.* **63**, 1499 (1989).